Theoretical Model Studies of the Iron Dimer Complex of MMO and RNR

Per E. M. Siegbahn

Department of Physics, Stockholm University, Box 6730, S-113 85 Stockholm, Sweden

Received November 18, 1998

Hybrid DFT calculations are used to study the structures and chemistry of the diiron complex of MMO and RNR. The chemical model used is larger than the ones used previously and contains the full first ligand sphere. New types of structures are suggested for the intermediates observed in the reactions of these enzymes. To obtain the very short Fe−Fe distances recently measured by EXAFS, it is suggested that both compound **Q** of MMO and compound **X** of RNR have two bridging carboxylates like the reduced diferrous complex but unlike the diferric complex. Antiferromagnetic coupling is shown to have significant effects on the electronic structure of the complexes and is also important for achieving the short Fe−Fe distance. The new model is also used to study the activation of methane, and a pure hydrogen abstraction transition state is located where a hydrogen of methane is abstracted by a bridging μ-oxo ligand. The combination of the methyl radical with the bridging μ-OH ligand formed occurs without a barrier and is extremely exothermic. This reaction should therefore be very fast. A symmetric transition state for the activation of O_2 is also proposed leading from a suggested compound **P** to compound **Q**. In this process, one of the carboxylate bridges of the reduced complex has to move away from O_2 toward one of the irons. These results are discussed in relation to recent experiments.

Introduction

The iron dimer complexes of methane monooxygenase (MMO) and ribonucleotide reductase (RNR) have attracted considerable interest during recent years and several reviews have appeared concerning different aspects of these complexes.[1−3] While MMO catalyzes the conversion of methane to methanol, RNR catalyzes the reduction of ribonucleotides to their corresponding deoxyribonucleotides. Although there are no obvious similarities between these reactions, the critical iron dimer complexes involved in these enzymes are very similar. In both, there are four carboxylates and two histidines, and in their oxidized forms, there are oxygen-derived bridging groups. The reduced form of the iron dimer complex of RNR can be schematically drawn as

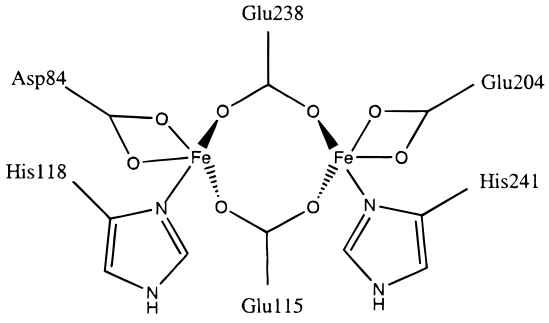

1

Apart from minor coordination differences, the corresponding complex of MMO differs only by the presence of a glutamic acid residue Glu114 at the position of the aspartate Asp84 of RNR. Since in the reduced form both irons have oxidation states II and there are four negative carboxylates and two neutral histidines, the entire complex is neutral. This is reasonable since the complexes are buried in the low dielectric medium of the protein where charge buildup will not easily occur. The net neutral charge will most likely persist also in the oxidized states of the complexes appearing in the catalytic cycles. The iron spins of these complexes are usually antiferromagnetically coupled, which means that the states with an even number of electrons are normally invisible in EPR. Exceptions to this rule are reduced MMO and some forms of reduced R2 of RNR, which have integer-spin EPR signals.[4,5]

The reduced complexes of both RNR and MMO are oxidized by a direct reaction with an oxygen molecule. Several intermediates in this reaction have been observed. One of these is a compound termed **P**,[4] which is invisible by EPR but has been studied by Mössbauer[6,7] and resonance Raman spectroscopies.[8] On the basis of these experiments, compound **P** has been suggested to be an Fe^{III}_2 peroxo complex. Suggested O_2 coordination modes are μ-η^2,η^2 (in plane or out of plane) and μ-η^1,η^1.

For MMO, compound **P** spontaneously converts to a species termed **Q**,[4,7] which is also invisible by EPR. On the basis of the Mössbauer spectrum for the enzyme from *M. trichosporium*, compound **Q** has been proposed to contain two Fe(IV) centers,[9] suggesting that this should be the first Fe^{IV}_2 dimer complex ever

(1) Feig, A. L.; Lippard, S. J. *Chem. Rev.* **1994**, *94*, 759.
(2) Wallar, B. J.; Lipscomb, J. D. *Chem. Rev.* **1996**, *96*, 2625.
(3) Andersson, K.; Gräslund, A. *Adv. Inorg. Chem.* **1995**, *43*, 359−408.
(4) Lee, S. K.; Nesheim, J. C.; Lipscomb, J. D. *J. Biol. Chem.* **1993**, *268*, 21569−21577.
(5) Froland, W. A.; Andersson, K. K.; Lee, S. K.; Liu, Y.; Lipscomb, J. D. *J. Biol. Chem.* **1992**, *267*, 17588−17599.
(6) Liu, K. E.; Valentine, A. M.; Wang, D. L.; Huynh, B. H.; Edmondson, D. E.; Salifoglou, A.; Lippard, S. J. *J. Am. Chem. Soc.* **1995**, *117*, 10174−10185.
(7) Liu, K. E.; Wang, D. L.; Huynh, B. H.; Edmondson, D. E.; Salifoglou, A.; Lippard, S. J. *J. Am. Chem. Soc.* **1995**, *116*, 7465−7466.
(8) Liu, K. E.; Valentine, A. M.; Qiu, D.; Wang, D. L.; Edmondson, D. E.; Appelman, E. H.; Spiro, T. G.; Lippard, S. J. *J. Am. Chem. Soc.* **1995**, *117*, 4997−4998. Resonance Raman data on **P** retracted in: *J. Am. Chem. Soc.* **1997**, *119*, 11134−11135.
(9) Lee, S.-K.; Fox, B. G.; Froland, W. A.; Lipscomb, J. D.; Münck, E. *J. Am. Chem. Soc.* **1993**, *115*, 6450−6451.

10.1021/ic981332w CCC: $18.00
Published on Web 05/19/1999

observed in biology. On the basis of a compilation of experiments,[10] of DFT calculations,[11] and of EXAFS measurements,[12] compound **Q** has been suggested to have a bis(μ-oxo) diamond core structure, **2**. The DFT calculations and the EXAFS

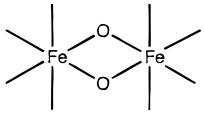

2

experiments independently suggested that this diamond core has substantially different Fe−O distances of 1.8 and 2.0 Å, which was explained by Jahn−Teller distortions with the weak axis of both irons being in the diamond core plane. In addition, the EXAFS results suggested an unusually short Fe−Fe distance for compound **Q** of only 2.46 Å.

For RNR, no complex corresponding to compound **Q** of MMO has yet been observed. Instead, the iron dimer with the highest oxidation states observed is another complex termed **X**.[13] This intermediate has been spectroscopically characterized as an $Fe^{IV}Fe^{III}$ dimer.[14] Recent EXAFS measurements again suggest, as in compound **Q** of MMO, a very short Fe−Fe distance of 2.5 Å.[15] ENDOR experiments have also been performed on compound **X**,[16] which, together with the EXAFS measurements, have led to the current best suggestion for **X**:

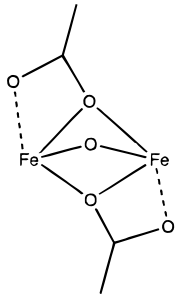

3

Since this structure has only one bridging μ-oxo and two monodentate bridging carboxylates, it is quite different from the diamond core structure previously suggested for **Q** and led to the suggestion that **Q** may also look like **3**. After **X** has been formed in RNR, the next step is the formation of the Tyr122$^{\bullet}$ tyrosyl radical which is close to the iron dimer center in the R2 protein. As this radical is formed, the iron dimer is reduced to the resting diferric Fe^{III}_2 dimer. When the ribonucleotide substrate arrives in the R1 protein, about 35 Å away from Tyr122, the radical is transferred to the substrate site[17] and the set of reactions start which transform the ribonucleotide to the deoxyribonucleotide.[18,19] After these reactions are completed, the radical returns to Tyr122.[20] These RNR reactions will not be further discussed here.

The hydroxylation of hydrocarbons by MMO has been studied extensively experimentally, and several possible mechanisms have been suggested.[1,2] These mechanisms fall essentially into two categories, radical and nonradical mechanisms. In the radical mechanisms, the first step is a hydrogen abstraction from the hydrocarbon, while the nonradical mechanisms suggest a concerted pathway. Support for the hydrogen abstraction mechanism comes from the kinetic isotope effects (KIEs) observed for *M. trichosporium*, which are some of the largest KIEs observed in biology.[21] Further support for this mechanism comes from studies with chiral substrates. With chiral ethane (CH_3-CHDT) as the substrate, 35% inversion of the configuration was observed with *M. trichosporium* MMO,[22] which is most consistent with a substrate radical that is not entirely free but constrained in some way by the enzyme active site. Nearly identical results were obtained with *M. capsulatus*.[23]

Support for a concerted nonradical mechanism of MMO comes mainly from radical clock measurements. For *M. capsulatus*, very fast radical clocks were studied with results inconsistent with the intermediacy of free radical intermediates because the maximum radical lifetime allowed by the data is an unreasonably short 2.5×10^{-14} s.[24,25] Fast radical clocks with *M. trichosporium* MMO give a small amount of ring-opening products, consistent with a short but not unreasonable radical lifetime of ca. 8×10^{-12} s.[24,26]

Different possible mechanisms for hydrocarbon hydroxylation by MMO were discussed recently in several papers.[26−31] These papers discuss possible mechanisms to account for the apparently conflicting information from chiral substrates, KIEs, and radical clocks. An alternative is to postulate several competing mechanisms or that enzymes derived from different bacterial sources have different mechanisms. Other suggestions made are, for example, a formation of an iron−carbon bond[27] and a concerted pathway involving a four-center transition state.[30]

The present study is a direct continuation of the previous DFT study on MMO.[11] In that study, a simple model of the iron dimer complex was used. The actual ligands in **1** were replaced by

(10) Shteinman, A. A. *FEBS Lett.* **1995**, *362*, 5−9.
(11) Siegbahn, P. E. M.; Crabtree, R. H. *J. Am. Chem. Soc.* **1997**, *119*, 3103.
(12) Shu, L.; Nesheim, J. C.; Kauffmann, K.; Munck, E.; Lipscomb, J. D.; Que, L., Jr. *Science* **1997**, *275*, 515.
(13) Bollinger, J. M.; Tong, W. H.; Ravi, N.; Huynh, B. H.; Edmondson, D. E.; Stubbe, J. *J. Am. Chem. Soc.* **1994**, *116*, 8024−8032. Bollinger, J. M.; Tong, W. H.; Ravi, N.; Huynh, B. H.; Edmondson, D. E.; Stubbe, J. *J. Am. Chem. Soc.* **1994**, *116*, 8015−8023. Ravi, N.; Bollinger, J. M.; Huynh, B. H.; Stubbe, J.; Edmondson, D. E. *J. Am. Chem. Soc.* **1994**, *116*, 8007−8014.
(14) Sturgeon, B. E.; Burdi, D.; Chen, S.; Huynh, B.-H.; Edmondson, D. E.; Stubbe, J.; Hoffman, B. M. *J. Am. Chem. Soc.* **1996**, *118*, 7551−7557.
(15) Riggs-Gelasco, P. J.; Shu, L.; Chen, S.; Burdi, D.; Huynh, B. H.; Que, L., Jr.; Stubbe, J. *J. Am. Chem. Soc.* **1998**, *120*, 849−860.
(16) Burdi, D.; Willems, J.-P.; Riggs-Gelasco, P.; Antholine, W. E.; Stubbe, J.; Hoffman, B. M. *J. Am. Chem. Soc.* **1998**, *120*, 12910−12919.
(17) Siegbahn, P. E. M.; Eriksson, L.; Himo, F.; Pavlov, M. *J. Phys. Chem.* **1998**, *102*, 10622−10629.
(18) Stubbe, J. *J. Biol. Chem.* **1990**, *265*, 5330. Mao, S. S.; Holler, T. P.; Yu, G. X.; Bollinger, J. M.; Booker, S.; Johnston, M. I.; Stubbe, J. *Biochemistry* **1992**, *31*, 9733−9743.
(19) Siegbahn, P. E. M. *J. Am. Chem. Soc.* **1998**, *120*, 8417.
(20) Sjöberg, B. M. *Structure* **1994**, *2*, 793−796. Sjöberg, B.-M. *Struct. Bonding* **1997**, *88*, 139−173.
(21) Nesheim, J. C.; Lipscomb, J. D. *Biochemistry* **1996**, *35*, 10240−10247.
(22) Priestley, N. D.; Floss, H. G.; Froland, W. A.; Lipscomb, J. D.; Williams, P. G.; Morimoto, H. *J. Am. Chem. Soc.* **1992**, *114*, 7561−7562.
(23) Valentine, A. M.; Wilkinson, B.; Liu, K. E.; Komarpanicucci, S.; Priestley, N. D.; Williams, P. G.; Morimoto, H.; Floss, H. G.; Lippard, S. J. *J. Am. Chem. Soc.* **1997**, *119*, 1818−1827.
(24) Liu, K. E.; Johnson, C. C.; Newcomb, M.; Lippard, S. J. *J. Am. Chem. Soc.* **1993**, *115*, 939−947.
(25) Choi, S.-Y.; Eaton, P. E.; Hollenberg, P. F.; Liu, K. E.; Lippard, S. J.; Johnson, C. C.; Newcomb, M.; Putt, D. A.; Upadhyaya, S. P.; Xiong, Y. *J. Am. Chem. Soc.* **1996**, *118*, 6547−6555.
(26) Ruzicka, F.; Huang, D. S.; Donnelly, M. I.; Frey, P. A. *Biochemistry* **1990**, *29*, 1696−1700.
(27) Deeth, R. J.; Dalton, H. *J. Biol. Inorg. Chem.* **1998**, *3*, 302−306.
(28) Whittington, D. A.; Valentine, A. M.; Lippard, S. J. *J. Biol. Inorg. Chem.* **1998**, *3*, 307−313.
(29) Siegbahn, P. E. M.; Crabtree, R. H.; Nordlund, P. *J. Biol. Inorg. Chem.* **1998**, *3*, 314−317.
(30) Yoshizawa, K. *J. Biol. Inorg. Chem.* **1998**, *3*, 318−324.
(31) Shteinman, A. A. *J. Biol. Inorg. Chem.* **1998**, *3*, 325−330.
(32) Lipscomb, J. D.; Que, L., Jr. *J. Biol. Inorg. Chem.* **1998**, *3*, 331−336.

Scheme 1

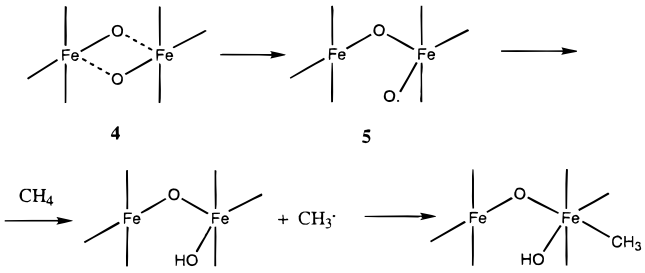

water and hydroxyl ligands to reproduce the desired oxidation states, maintaining an overall neutral model. This type of modeling was required to make the necessarily large number of quantum chemical investigations possible but also to simplify the conclusions made. Once the major effects have been characterized, the model can be extended and new effects identified. Although these model studies started with 6-coordinated iron centers, it was soon found that the complexes rearranged to 5-coordination. In most investigations, 5-coordinated irons were therefore used. One of the main results of the previous study was a suggested structure for compound **Q** as shown in **4**. An interesting feature of this Fe^{IV}_2 dimer is the

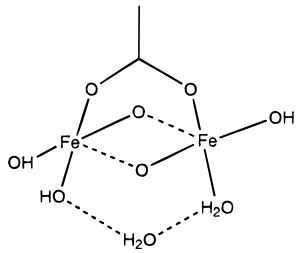

large difference between the diamond core Fe−O distances, already mentioned above. Another significant finding is that it is energetically possible for this Fe^{IV}_2 dimer to abstract hydrogen from methane in line with the hydrogen abstraction model suggested on the basis of experiments on chiral substrates and KIEs. A linear O−H−C structure was obtained for the transition state without any tendency for a concerted four-center transition state, even though the transition state search was started from such a structure. For model **4** to activate methane, it was found that it had to rearrange according to Scheme 1 to structure **5** with a single iron-based oxyl radical. The rearrangement barrier from **4** to **5** was assumed to be small, and the hydrogen abstraction using **5** was found to have a low barrier of 6.3 kcal/mol compared to the lowest iron dimer isomer. After the transition state was passed, leading to a free methyl radical, it was found that the methyl radical moved to form a weak Fe−C bond at the empty coordination site on the active iron, which was suggested to be a possible explanation for the short radical lifetime as measured by radical clocks. The hydroxyl and methyl ligands finally combined to form methanol. Different isomers were obtained in the geometry optimizations, and possible identifications with the intermediates observed experimentally were made.

It is clear that, with such a model as simple as **4**, the different suggestions made in that study have to be tested by more realistic models. For this reason, the present study was made at the next natural level of modeling the iron dimer complex. At this level, all the amino acid side chain carboxylates and imidazoles in the first coordination shell are included in the model as in **1**. This is most certainly not the final level of theoretical modeling, and in a not too distant future, the second-shell ligands will probably also be included in some way in the modeling. However, the first-shell modeling should represent a significant advancement with respect to the previous simple model and many of the issues raised for MMO and RNR could be tested on much firmer ground than with the previous model.

Computational Details

The calculations were performed in three steps. Following an optimization of the geometry using medium-size basis sets, the energy was evaluated using large basis sets. In the third step, the effect of the polarized surrounding was evaluated. All these steps were made at the B3LYP level[33,34] using the GAUSSIAN-94 program.[35]

In the B3LYP geometry optimizations, standard double-ζ basis sets were employed. For the metal-containing systems, the LANL2DZ set (from Gaussian 94) was used. This basis set uses an ECP (effective core potential)[36] for the metal atoms. These rather small basis sets can safely be used for the present purposes since it has been clearly shown that the final energy is very insensitive to the quality of the geometry optimization.[37,38] The B3LYP final energy calculations were made using larger basis sets where the LANL2DZ basis set was extended by adding diffuse functions and a single set of polarization functions for all atoms taken from the 6-311+G(1d,1p) basis set.

The dielectric effects from the surrounding protein were obtained using the self-consistent isodensity polarized continuum model (SCI-PCM) as implemented in the Gaussian 94 program.[35,39] In this method, the cavity is defined self-consistently in terms of a surface of constant charge density for the solute molecule. The default isodensity value of 0.0004 e/B^3 was used. The dielectric constant ϵ of the protein is the main empirical parameter of the model, and it was chosen to be equal to 4, in line with previous suggestions for proteins. This value corresponds to a dielectric constant of about 3 for the protein itself and of 80 for the water medium surrounding the protein. The choice of $\epsilon = 4$ was recently shown to give good agreement with experiment for three different electron transfer processes in the bacterial photosynthetic reaction center.[40] It should be noted that the present systems are much less sensitive to the choice of ϵ since the charge separations are only minor and, overall, almost negligible dielectric effects were obtained.

Since the present model systems are quite large by quantum chemical standards, the effects of zero-point vibration cannot be directly calculated but have to be estimated. Differential zero-point effects are assumed to be small and set to zero when forms of the same complex are compared. When bonds are formed as in the substrate reaction of MMO, the zero-point effects are taken from the previous study using smaller model complexes.[11] It should finally be added that, for some complexes discussed below, calculations are performed for antiferromagnetic coupling of the metal spins, where the use of DFT leads to

(33) Becke, A. D. *Phys. Rev. A* **1988**, *38*, 3098. Becke, A. D. *J. Chem. Phys.* **1993**, *98*, 1372. Becke, A. D. *J. Chem. Phys.* **1993**, *98*, 5648.
(34) Stevens, P. J.; Devlin, F. J.; Chablowski, C. F.; Frisch, M. J. *J. Phys. Chem.* **1994**, *98*, 11623.
(35) Frisch, M. J.; Trucks, G. W.; Schlegel, H. B.; Gill, P. M. W.; Johnson, B. G.; Robb, M. A.; Cheeseman, J. R.; Keith, T.; Petersson, G. A.; Montgomery, J. A.; Raghavachari, K.; Al-Laham, M. A.; Zakrzewski, V. G.; Ortiz, J. V.; Foresman, J. B.; Cioslowski, J.; Stefanov, B. B.; Nanayakkara, A.; Challacombe, M.; Peng, C. Y.; Ayala, P. Y.; Chen, W.; Wong, M. W.; Andres, J. L.; Replogle, E. S.; Gomperts, R.; Martin, R. L.; Fox, D. J.; Binkley, J. S.; Defrees, D. J.; Baker, J.; Stewart, J. P.; Head-Gordon, M.; Gonzalez, C.; Pople, J. A. *Gaussian 94*, Revision B.2; Gaussian Inc.: Pittsburgh, PA, 1995.
(36) Hay, P. J.; Wadt, W. R. *J. Chem. Phys.* **1985**, *82*, 299.
(37) Bauschlicher, C. W., Jr.; Ricca, A.; Partridge, H.; Langhoff, S. R. In *Recent Advances in Density Functional Methods*; Chong, D. P., Ed.; World Scientific Publishing Co.: Singapore, 1997; Part II, p 165.
(38) Siegbahn, P. E. M. *Adv. Chem. Phys.* **1996**, *93*, 333.
(39) Wiberg, K. B.; Rablen, P. R.; Rush, D. J.; Keith, T. A. *J. Am. Chem. Soc.* **1995**, *117*, 4261. Wiberg, K. B.; Keith, T. A.; Frisch, M. J.; Murcko, M. *J. Phys. Chem.* **1995**, *99*, 9072.
(40) Blomberg, M. R. A.; Siegbahn, P. E. M.; Babcock, G. T. *J. Am. Chem. Soc.* **1998**, *120*, 8812−8824.

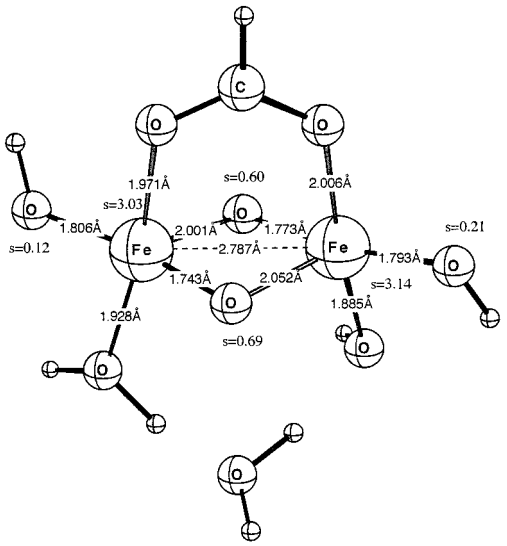

Figure 1. Previous simple model for compound **Q** with one bridging carboxylate. The structure was obtained using ferromagnetic spin coupling (^{9}A).

significant spin contaminations. However, for the cases discussed below, the energetic gain by the antiferromagnetic coupling is sufficiently small that the energies should be reasonable.

Results and Discussion

Several intermediates in the enzyme reactions of MMO and RNR have been observed, as discussed in the Introduction. Some of these were assigned in the previous study on MMO. In the first subsection below, these assignments are discussed again for the new larger model including the full first ligand sphere. New experimental information for these intermediates is also considered in the analysis. In particular, the implications of the surprisingly short Fe−Fe distances obtained for both compound **Q** and compound **X** using EXAFS are discussed. When different possible models of the intermediates are discussed, the relative energies become important, and certain aspects of this are discussed in the second subsection. In the third subsection, the activation of methane in MMO is discussed for the new larger model, and in the fourth subsection, the activation of O_2 is discussed. These reactions must be considered as very difficult to treat quantum chemically, and the results obtained should be regarded as suggestions that should stimulate further investigations rather than as final conclusions.

a. Models for Observed Intermediates. One of the main results in the previous study on MMO was an assignment of the structure for compound **Q** as shown in Figure 1. This structure was obtained using ferromagnetic spin coupling and was a result of some preliminary investigations of different simple models. One striking feature of this structure is the quite different Fe−O distances of the diamond core, with two short bonds of 1.74 and 1.77 Å and two longer ones of 2.00 and 2.05 Å. This was explained by the presence of Jahn−Teller (JT) distortions with the weak JT axis going through the long Fe−O bond on one side of the iron atoms and with an empty site on the other side, leading to 5-coordinations for the irons. The Fe−Fe distance is 2.79 Å, which is quite short but not as short as the 2.46 Å distance measured by EXAFS. This discrepancy suggests that some feature of the bonding may have been missing in the previous model, and this question is the first one to be analyzed here.

Using a simple iron dimer model, several new possible structures for compound **Q**, not thought of in the previous study,

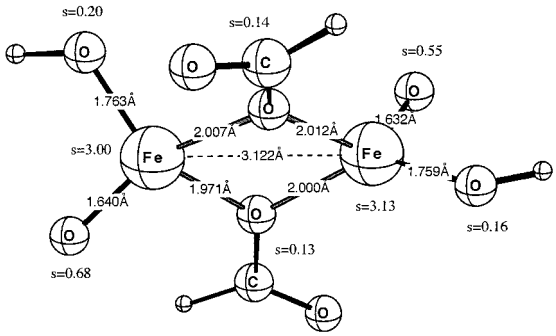

Figure 2. Model for compound **Q** with two monodentate bridging carboxylates. The structure was obtained using ferromagnetic spin coupling (^{9}A).

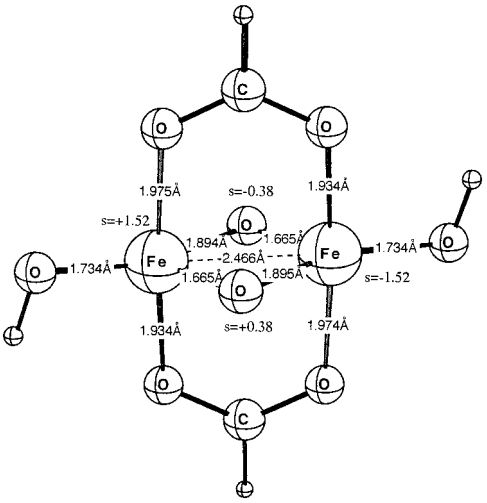

Figure 3. New simple model for compound **Q** with two bridging carboxylates. The structure was obtained using antiferromagnetic spin coupling (^{1}A).

were investigated. One of these structures is shown in Figure 2 and was designed to mimic the new suggestion made on the basis of recent EXAFS and ENDOR studies.[15] The model differs from the previous one by having two carboxylates rather than one. These carboxylates were placed as monodentate, and in the starting structure for the optimization, one of the oxygens was bridging as in **3**. To obtain an Fe^{IV}_2 dimer and stay with a neutral model, this requires one terminal oxo ligand. As the optimization progressed, the bridging oxygen moved out, and in the final structure in Figure 2, there are two terminal oxo ligands instead of one. The spins on iron are about 3.0, which is characteristic for Fe(IV) using weak-field ligands and ferromagnetic spin coupling. Rather than making the Fe−Fe bond shorter, the new structure has a substantially longer bond of 3.12 Å. Even though antiferromagnetic spin coupling and other modifications of the model may shorten the Fe−Fe bond, it was considered as a less promising candidate for **Q** than other models.

The most interesting possible structure for compound **Q** of the new simple models tried is shown in Figure 3. This was actually the first new model tried and was chosen on the basis of the intuition that bridging carboxylates should prefer parallel Fe−O(carboxylate) bonds. In the old structure in Figure 1, it appears that the $H_2O\cdot\cdot HOH\cdot\cdot OH$ bridge forces the irons somewhat apart in order to accommodate the hydrogen bonds. Parallel Fe−O(carboxylate) bonds could lead to a reduction of the Fe−Fe distance since the O−O distance of a carboxylate is only 2.31 Å. This assumption was confirmed to some extent,

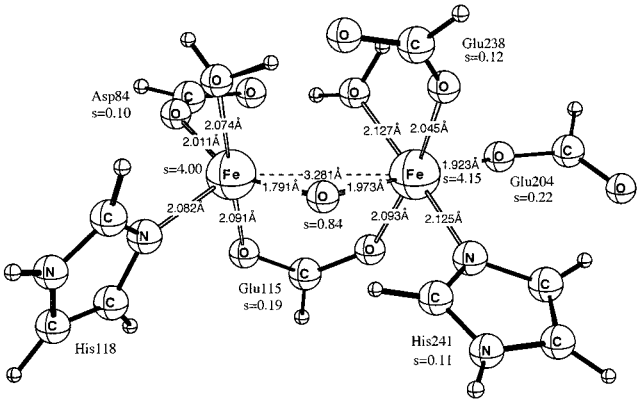

Figure 4. Resting diferric state of RNR. The structure was obtained using ferromagnetic spin coupling (^{11}A).

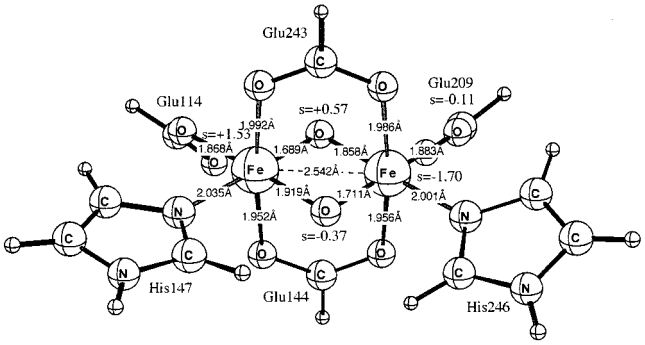

Figure 5. Suggested model for compound **Q** of MMO with two bridging carboxylates. The structure was obtained using antiferromagnetic spin coupling (^{1}A).

and with two bridging carboxylates the bond decreased from 2.79 to 2.74 Å, still using ferromagnetic spin coupling. Keeping the same structure but using a somewhat larger basis set in the geometry optimization with d functions on oxygen led to a further shortening of the Fe−Fe distance by 0.07 Å to 2.67 Å. In the final attempt to make the Fe−Fe bond still shorter, antiferromagnetic spin coupling was used. This is much more difficult to converge, but after some effort, the proper spin coupling was achieved. Still using d functions on oxygen, the optimization converged to the structure in Figure 3 with a short Fe−Fe distance of 2.47 Å in fortuitously good agreement with the EXAFS experiment. The effect of the antiferromagnetic spin coupling is thus a shortening by as much as 0.20 Å.

As seen from the spin populations given for the old structure in Figure 1 and the new structure in Figure 3, the spin distributions in these complexes are quite different. The difference cannot be just described in terms of ferro- and antiferromagnetic spin couplings; there are also other differences. The major difference is that the spins on iron are substantially reduced from about 3.0 to 1.5, but the spin is also much more spread out on the ligands for the ferromagnetic coupling case. The spins are less than 0.1 (not marked in the figure) on all ligands in Figure 3 except on the oxygens, which have a spin of 0.38. The low spin is indicative of additional covalency in the bonding for the antiferromagnetic case. The diamond core distances are also reduced to 1.67 and 1.89 Å, respectively. The JT distortions are still quite noticeable although not as pronounced as for the ferromagnetic case.

The first structure optimized using the full first ligand sphere was the resting diferric state of RNR; see Figure 4. The experimental X-ray structure[41] was used as a starting point for the optimization. Ferromagnetic spin coupling was used since all attempts to obtain convergence to a reasonable state using antiferromagnetic coupling failed. The main features of the experimental structure are well reproduced by the calculation concerning, for example, bond directions and rough bond distances. For most of the distances, the calculated results are within the experimental error bars, which are as large as 0.2−0.4 Å, as indicated by the differences of the experimental values for the two supposedly identical subunits. It is likely that, to obtain very accurate calculated structures (errors of less than 0.1 Å), both a larger basis set and a model with antiferromagnetic coupling that includes also the second-sphere ligands are needed, but this belongs to the next level of modeling. At the present stage, it is considered unlikely that second-sphere ligands should seriously affect the chemistry of the model complex unless these particular ligands are directly involved in bond forming or bond breaking. One possible such case will be discussed below.

The bridging oxygen in the diferric complex in Figure 4 probably comes from the oxygen molecule that has reacted with the reduced diferrous complex, leading first to compound **P** and then to compound **Q** (in MMO). The second oxygen is most likely in one of the water molecules coordinating to the irons. Due to the high symmetry of the complex, it is very difficult to say in which one of these water molecules the oxygen ends up. Assuming that it is in the left one in Figure 4, removing the hydrogen atoms from this water and moving this oxygen between the iron atoms lead to a structure that was used as a reasonable starting structure for compound **Q**. Once the optimization started, the first event was that Glu238 felt the empty coordination site on the other iron (left by the water molecule) and began to bind to this position. This quickly led to a type of structure similar to the one in the simple model complex in Figure 3 with two bridging carboxylates. This shows that to go between compound **Q** and the resting diferric complex requires a minimum of structural rearrangement and is thus another reason a structure with two bridging carboxylates appears as a reasonable suggestion for compound **Q**. The optimization eventually led to a structure where the second water molecule, the one on the iron atom to the right in Figure 4, moved out into the second coordination shell. In order not to complicate the further studies of different intermediates by having to investigate possible hydrogen-bonding situations for this water molecule, it was removed from the model at this point. It must finally be emphasized that many of the reactions discussed in this paragraph are theoretical constructs to achieve structures of the desired type. For example, the resting diferric state has been observed in RNR while compound **Q** has only been observed in MMO.

When the water molecule on the iron atom to the right of the diferric structure in Figure 4 was removed and antiferromagnetic spin coupling was used, the geometry optimization converged to the structure in Figure 5. The basis set used in this optimization included d functions on the oxygens as did the basis set used to obtain the structure in Figure 3. Further extensions of the basis set, such as including d functions on nitrogen and diffuse functions on oxygen, did not change the Fe−Fe distance or any of the distances in the diamond core (less than 0.01 Å). The structure in Figure 5 is the best suggestion for compound **Q** that can be made on the basis of the present calculations. The Fe−Fe distance of 2.54 Å is reasonably close to the experimental EXAFS distance of 2.46 Å considering the model used and the fact that, for example,

(41) Nordlund, P.; Sjöberg, B.-M.; Eklund, H. *Nature* **1990**, *345*, 593−598.

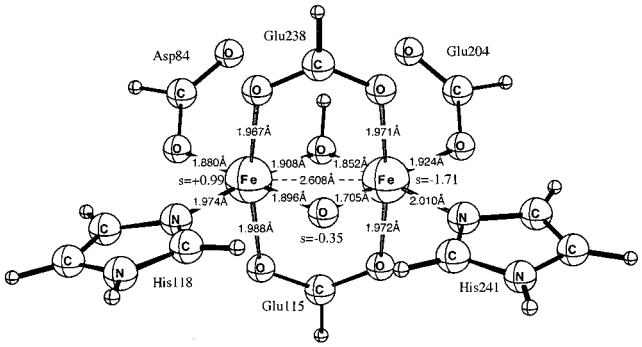

Figure 6. Suggested model for compound **X** of RNR with two bridging carboxylates. The structure was obtained using antiferromagnetic spin coupling (^{2}A).

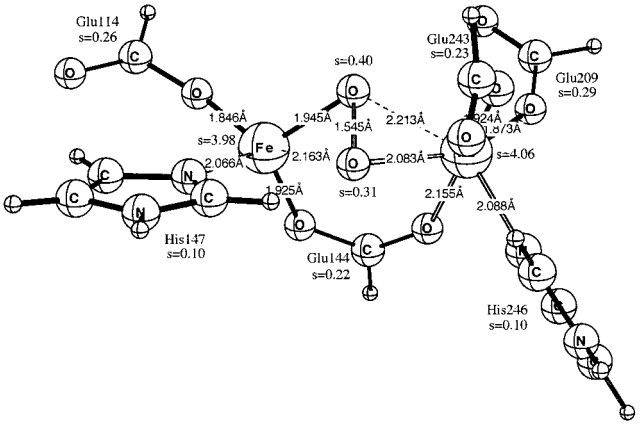

Figure 7. Optimized peroxo state. The structure was obtained using ferromagnetic spin coupling (^{11}A).

relativistic effects are not included. It is first important to note that the structures of the simple model in Figure 3 and the more advanced one in Figure 5 have many similarities, which supports the use of the simple models in the previous study. Even though the symmetry is lower, both irons are 6-coordinated, and some of the ligands are nitrogen derived for the larger model, the JT distortions are, for example, quite similar. The spin distribution is also quite similar, but the asymmetry of the complex causes the oxygen trans to the histidines to obtain a somewhat higher spin, +0.57 compared to −0.37, which should make it more reactive. Since this oxygen is the one pointing toward the substrate pocket in MMO, this could be an important effect. Again, as in the simple model, the antiferromagnetic spin coupling causes a significant reduction of the spins on the irons and on the ligands compared to the ferromagnetic case. A few comments can finally be made on the structure of the ferromagnetic coupling case (not shown) for the model in Figure 5. The Fe−Fe distance is 2.82 Å, showing an effect of ferromagnetic coupling similar to that in the small model. The differences in the Fe−O diamond core distances are very pronounced, with two short distances of 1.69 and 1.72 Å and two long ones of 2.14 and 2.16 Å. It should be noted that these distances were obtained using a somewhat smaller basis set (without polarization functions on oxygen) than the one used for the structure in Figure 5.

Another type of structural model, more in line with structure **3**, was also tried for compound **Q**. In this model, one of the bridging carboxylates was chosen as a monodentate ligand and one of the oxygens as a terminal oxo ligand. Using ferromagnetic coupling, this modification led to an Fe−Fe distance which is 0.30 Å longer than that for the ferromagnetic coupling case of the structure in Figure 5 and to an energy which is about 10 kcal/mol higher. This model study thus gave the same indication as the one using the simple model structure **2**, that monodentate bridging carboxylates do not lead to the desired shortening of the Fe−Fe distance but, on the contrary, to significantly longer distances and less favorable energies.

Since compound **X** was found by EXAFS to have a short Fe−Fe bond distance similar to that in compound **Q**, it seems reasonable to assume a similar structure for **X** with two bridging carboxylates. To maintain a neutral complex (see Introduction), a hydrogen atom should be placed somewhere on the compound **Q** structure. The most obvious place to put this hydrogen is on a bridging oxygen. Since the substrate pocket of MMO is trans to the histidines, the hydrogen was placed on this oxygen. This led to an optimized structure for a suggested compound **X** shown in Figure 6. The Fe−Fe distance in this structure of 2.61 Å is only 0.07 Å longer than the one obtained for compound **Q** at the same level of treatment, which appears to be in reasonable agreement with the observation that the Fe−Fe distances should be similar, considering uncertainties in both calculations and experiments. Again, polarization functions on oxygen were used. The spin distributions of compounds **Q** and **X** are quite similar apart from the obvious result that the spin has disappeared on the bridging oxygen that binds the additional hydrogen in **X**. The spin on the Fe(III) iron of this $Fe^{III}Fe^{IV}$ complex is also reduced from +1.53 to +0.99.

The structures suggested here for **X** and **Q** are quite different from the one (structure **3**) given as the best suggestion recently based on EXAFS and ENDOR experiments.[15] However, it should be noted that the present structures are quite consistent with the bond distance information obtained from EXAFS and cannot be excluded on the basis of those experiments. The interpretations of the ENDOR experiments suggest that there is only one bridging oxygen. However, in the structure in Figure 6, the bridging μ-oxo ligand is substantially closer to one of the irons and the possibility that this could be interpreted as a ligand on only one of the irons should also be considered. Also, from the ENDOR measurements it was found that only one of the oxygens of O_2 is exchangeable with water in compound **X**. This observation is also consistent with the structure in Figure 6, where the bridging hydroxyl group should be easily exchangeable but not the bridging μ-oxo group. The very unusual spin distribution shown in Figures 5 and 6 for these complexes, indicating strong covalencies in the antiferromagnetic case, is another reason ENDOR interpretations could be quite difficult, suggesting that also the type of quadruply bridging complexes found in the present optimizations should be considered as possible models for the interpretations, which appears not to have been the case before. Finally, it must be emphasized that, in the present study, it has been assumed that the complexes are neutral (see motivation for this in the Introduction). The possibility that compound **X** is actually charged should be taken into consideration in future studies. Investigations of this type are in progress.

From the present model calculations, it is suggested that both compounds **X** and **Q** have two bridging carboxylate groups like the reduced diferrous complex **1**. This type of structure is not possible for the intermediate peroxo structure, compound **P**. To make place for an oxygen molecule, one of the carboxylates has to be displaced, and the best structure found here is the one shown in Figure 7. This structure has the peroxo group rather symmetrically placed between the irons, with the midpoint (M) of O_2 forming an Fe−M−Fe bond angle of 132°. This bonding mode is quite similar to the one found in calculations recently

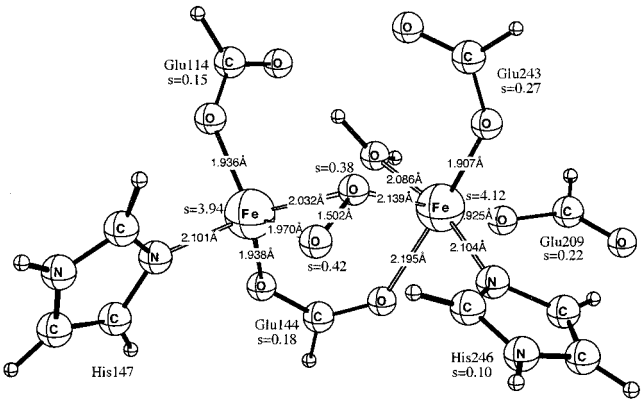

Figure 8. Alternative peroxo state. The structure was obtained using ferromagnetic spin coupling (^{11}A).

for a model of the copper dimer peroxo complex of tyrosinase.[42] The structure in Figure 7 is not the only possible structure for compound **P**. In an optimization keeping a water molecule in the first coordination sphere, the structure shown in Figure 8 was obtained. This water molecule is the same one found in the experimental structure of the resting diferric state; see Figure 4. The coordination of the water to one of the irons blocks the symmetric position of the oxygen molecule. Instead, the oxygen molecule has one of its oxygens symmetrically bound between the irons and the other oxygen bound only to one iron, which is the same type of peroxo structure found in the previous computational MMO study. A similar asymmetric binding of a substrate to the iron dimer complex was recently also found in an X-ray structure with an azide substrate.[43] Purely on the basis of the present model calculations, it is difficult to conclude which of the peroxo structures in Figures 7 and 8 should be most favorable in the actual enzyme. This conclusion must be based also on other types of indirect spectroscopic information. In resonance Raman experiments where O_2 containing one ^{16}O and one ^{18}O was used, only a single band was observed, indicating a symmetric structure.[2,8] In addition, in Mössbauer experiments only a single quadrupole doublet was observed, again suggesting that both oxygens are bound symmetrically to the irons.[8] For this reason, and from reasons given below concerning the activation of O_2, the structure shown in Figure 7 is here suggested as the best candidate for the actually observed compound **P**. It should be noted again that this structure was obtained using ferromagnetic coupling, which may cause minor errors. However, the errors should be much smaller for this complex, which has a large Fe−Fe distance of 3.58 Å, than the corresponding errors for compounds **Q** and **X**, with much shorter Fe−Fe distances. In a recent study of a bis(μ-oxo) manganese dimer, the geometrical parameters for the ferromagnetic and antiferromagnetic structures were found to be virtually identical.[44]

b. Energetic Considerations. As discussed above, several different spin states appear in the assignment of the intermediates observed for MMO and RNR. Although B3LYP is the most reliable DFT method at present for considering relative energies, certain systematic errors are likely to appear. During the course of the present study, it became increasingly clear that B3LYP slightly favors high-spin states compared to lower spin states. This does not appear to be a severe problem for spin multiplicities lower than 9 but gradually becomes more serious for higher spin multiplicities and has to be taken into account when the reactions are discussed. The unbalanced treatment of different spin states is a much more severe problem for nonhybrid methods, where Hartree−Fock exchange is not included, and for these methods quite unreliable relative energies can be obtained for the present type of complexes.[45] The solution to this problem has not been found yet, but this is an area of intense research at present.

There are a few cases where comparisons to experiments indicate that high-spin states are favored by B3LYP. The first case is the comparison between ferro- (^{9}A) and antiferromagnetic (^{1}A) coupling of compound **Q**, where the latter coupling is known experimentally to be favored. At the B3LYP level, the antiferromagnetic coupling is favored but not by more than 0.3 kcal/mol, which does not appear to be enough. Some further stabilization could come from extensions of the basis set since going from the small (LANL2DZ) to the larger basis set increased the relative stabilization of the antiferromagnetic coupling by 1.9 kcal/mol. The B3LYP favoring of high-spin states is more obvious for compound **X**, which is also known to be antiferromagnetically (^{2}A) coupled but where B3LYP favors the ferromagnetic coupling (^{10}A) by as much as 5.9 kcal/mol. Also, in the comparison of the present models for compounds **P** and **Q**, the favoring of high spin is clear. Experimentally, the O−O bond-breaking reaction leading from **P** to **Q** should be exothermic, but the B3LYP energies give an endothermic reaction by as much as 8.8 kcal/mol. This energy is obtained upon going from the ferromagnetically coupled **P** (^{11}A) to the antiferromagnetically coupled **Q** (^{1}A). In the previous model study,[11] a similar problem was noted in comparing **P** and **Q**, and the results indicated that the energy difference could decrease by as much as 5 kcal/mol upon going to a larger basis set than used in the present study. Still, it is clear that relative B3LYP energies involving comparisons of different spin states with spin greater than 9 have to be taken with caution. Comparisons of energies for states with the same spin should be more reliable.

c. Methane Activation in MMO. In the previous study of methane activation in MMO, simple ligands were used; see Figure 1. One consequence of using these ligands was that the complex rearranged in the geometry optimization and 5-coordination was preferred even if the optimization was started with 6-coordinated metals. This does not occur for the present more realistic modeling, and the iron atoms remain 6-coordinated for compound **Q**. One reason for this is that the water ligands used previously form strong second-sphere hydrogen bonds, which are competitive with direct metal−water bonds. Nevertheless, the relative energies were not very different from the ones obtained here (see above) and important general results could still be drawn from the previous study. However, it is clear that some of the aspects of the previous mechanism as shown in Scheme 1 have to be reconsidered since the empty coordination site played a role in this mechanism. In this subsection, the activation of methane will therefore be studied again using the larger model.

The presently suggested model for compound **Q** in Figure 5 has considerably less coordination flexibility than the previous one in Figure 1. If the doubly bridging carboxylates are retained during the reaction, there are not many places on the complex

(42) Lind, T.; Siegbahn, P. E. M.; Crabtree, R. H. *J. Phys. Chem.* **1999**, *103*, 1193−1202.
(43) Andersson, M. E.; Högbom, M.; Rinaldo-Matthis, A.; Andersson, K. K.; Sjöberg, B.-M.; Nordlund, P. *J. Am. Chem. Soc.* **1999**, *121*, 2346−2352.
(44) Blomberg, M. R. A.; Siegbahn, P. E. M.; Styring, S.; Babcock, G. T.; Åkermark, B.; Korall, P. *J. Am. Chem. Soc.* **1997**, *119*, 8285.
(45) Siegbahn, P. E. M.; Blomberg, M. R. A. *Annu. Rev. Phys. Chem.*, submitted for publication.

where a methane molecule could be activated. The most plausible place for activation is the μ-oxo bridge trans to the histidines. This is close to the hydrophobic pocket in the protein to which methane can diffuse and in which it will fit. As seen from the spin populations in Figure 5, the spin on the μ-oxo ligand trans to the histidines is also higher than that on the other μ-oxo ligand, which should make it more reactive. This could be one role of the histidines. A transition state for methane activation was approached by freezing the distance at different values between the oxygen and the closest of the hydrogens on methane. Full geometric freedom was otherwise given, which means that both a hydrogen abstraction and a more concerted pathway involving, for example, oxygen insertion are allowed. The search for a transition state was initiated on the antiferromagnetic ^{1}A ground state of compound **Q**, but no tendency toward C−H activation was noted. As the O−H distance was frozen to smaller values, the energy just increased. Several other spin states (^{3}A, ^{5}A, etc.) were then investigated with the same negative result until the ferromagnetic ^{9}A state was tried. On this surface, there is a smooth activation of methane, and the fully optimized transition state is shown in Figure 9. The barrier obtained using the large basis set and including estimated zero-point vibrational effects is 7.1 kcal/mol on this surface. Since the reaction occurs on the ferromagnetic ^{9}A potential surface and the ground state is the antiferromagnetic ^{1}A state, it is required for this mechanism that the promotion energy to reach the ^{9}A state not be high. As discussed in the previous subsection, the calculated value for this promotion energy of only 0.3 kcal/mol is probably underestimated by a few kcal/mol, which means that the best prediction that can be made for the barrier of activating methane should be in the range 10−12 kcal/mol. Uncertainties of the B3LYP method for transition states and basis set incompleteness are not taken into account since they are difficult to estimate. Apart from the requirement of a small promotion energy to reach the ^{9}A state, the fact that a transition to another surface is needed should not be a problem since spin−orbit coupling in these systems is strong. The reason the reaction is easier on the ferromagnetic surface is that there is a considerable covalency in the Fe−O bonds of the antiferromagnetic state that needs to be broken up for the reaction with methane. The reaction leads to a methyl radical and compound **X** in Figure 6. The calculated exothermicity is 2.3 kcal/mol. Since the calculated C−H bond strength of methane is 104.2 kcal/mol (experimental 103.3 kcal/mol), this exothermicity corresponds to an O−H bond strength for compound **X** as high as 106.5 kcal/mol. Considering the uncertainties involved in, for example, comparing different spin states, it is quite possible that this hydrogen abstraction reaction could also be slightly endothermic.

The transition state shown in Figure 9 is clearly one of an almost pure hydrogen abstraction. It is important to note that this was not forced on the geometry optimization by any constraint. A pure hydrogen abstraction mechanism was also found in the previous study on MMO even though the complex was much simpler and the abstraction was made by a terminal oxo ligand rather than by a bridging one. Furthermore, in the previous study, the geometry optimization was started as a four-center transition state similar to the one found in a study on a naked FeO^+ model[30] and still converged to pure hydrogen abstraction. There are two major differences between the FeO^+ model and the present model. First, the cationic charge of FeO^+ leads to a strong electrostatic attraction to molecular methane of 19.5 kcal/mol. It should be noted that molecular minima on neutral, coordinatively unsaturated complexes are found, but

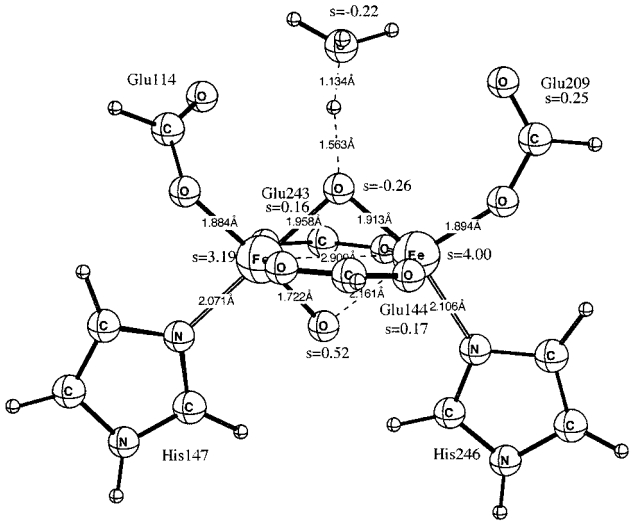

Figure 9. Optimized transition state for CH_4 activation in MMO. The structure was obtained using ferromagnetic spin coupling (^{9}A).

always with much smaller binding energies.[46] The deepest minima for neutral complexes have furthermore been found for cases with strong ligand fields and low spins on the metal, in contrast to the present cases of weak ligand fields and high spin on the metals (also in the case of antiferromagnetic coupling). For the present and the previous model (which is coordinatively unsaturated), several types of possible molecular methane structures were investigated but no minima were found. The second major difference between the models is that FeO^+ is unsaturated, which allows undisturbed formation of an Fe−C bond, leading to a strongly exothermic reaction by 40.9 kcal/mol in contrast to the present result of only 2.3 kcal/mol. In another study by the same authors[47] a more realistic iron dimer model of compound **Q** was used. This model has one 4-coordinated and one 5-coordinated iron atom, and the complex has a total charge of +3. A four-centered transition state similar to the one for FeO^+ was found also on this larger model. The positive charge again leads to a deep molecular methane minimum on the 4-coordinated iron of 27.3 kcal/mol, even deeper than that for FeO^+, and the barrier for methane activation is 31.6 kcal/mol using the B3LYP method. These results are thus completely different from the present ones, and the differences are again explained by the large electrostatic attraction, absent in the present model, and the unsaturated metal atoms. The present quantum chemical models are therefore expected to be much more appropriate for the enzyme than the the charged FeO^+ model.

Although there were no constraints in the final optimization of the transition state for methane activation, the search for a transition state different from one of pure hydrogen abstraction was continued. For example, starting from the methanol product and going backward toward the reactants shortening the C−H bond in steps. This was done both on the ferromagnetic ground state potential surface for the methanol product, which is ^{11}A (see below), and on the ferromagnetic ground state potential surface for compound **Q**, which is ^{9}A. This leads to a reaction pathway of the oxygen insertion type with short O−H and O−C distances. As the C−H bond was shortened, there was no tendency toward methane formation but the energy just in-

(46) Yoshizawa, K.; Shiota, Y.; Yamabe, T. *Organometallics* **1998**, *17*, 2825−2831.
(47) Yoshizawa, K.; Ohta, T.; Shiota, Y.; Yamabe, T. *Chem. Lett.* **1997**, 1213−1214; *Bull. Chem. Soc. Jpn.* **1998**, *71*, 1899.

creased, indicating a quite high barrier on both surfaces. Another type of hydrogen abstraction involving one of the oxygens on the glutamates, Glu114 and Glu209, rather than a μ-oxo oxygen was also tried, on both a ^{9}A and an ^{11}A surface. Again, the barrier was found to be much higher than the one found for the pathway in Figure 9. It should also be noted that a concerted pathway involving both the μ-oxo oxygens, as suggested in other work,[31] is not possible using the present model of **Q** for steric reasons, unless a costly opening of one of the carboxylate bridges is made prior to the methane activation. This type of pathway was therefore not tried.

After the transition state in Figure 9 is passed, a free methyl radical is formed. This radical can then without any barrier combine with the bridging μ-OH group to form methanol. The methanol product is an Fe^{III}_2 complex, which with ferromagnetic coupling leads to an ^{11}A state. Since the ferromagnetic state of compound **Q** is ^{9}A, there must be a spin change somewhere along this reaction. The reaction is calculated to be exothermic by as much as 63.0 kcal/mol. Since this value appears quite large, a few additional calculations were performed. First, the reaction between molecular oxygen and methane to form methanol and a free oxygen atom

$$CH_4 + O_2 \rightarrow CH_3OH + O(^3P) \qquad (1)$$

is calculated to be endothermic by 30.3 kcal/mol (experimental 29.7 kcal/mol). On the left-hand side of (1) are the starting substrate reactants of MMO, which form very weak van der Waals bonds to the reduced diiron complex. To form the products of the methanol formation in MMO on the right-hand side, methanol should be bound to the diferric iron complex and the oxygen atom as a bridging μ-oxo oxygen. The calculated values for these two binding energies are 18 and 62 kcal/mol, respectively. This gives a total exothermicity for the substrate reaction of MMO of 50 kcal/mol. The formation of the methyl radical by compound **Q** and methane is slightly exothermic by 2 kcal/mol. The final reaction of interest here is the reaction between the oxygen molecule and the reduced diferrous complex. Since this is a very complicated reaction where a large number of bonds are formed and broken, only a very approximate reaction energy can be obtained. The calculations turn out to give an endothermic reaction by 16 kcal/mol, which is somewhat surprising. Summing these values leads back to the 63 kcal/mol exothermicity of the combination reaction between a methyl radical and compound **X**. Since the endothermic value for the O_2 reaction is surprising, this value was recalculated with a still larger basis set with two polarization functions on each atom rather than one, but this only changed the endothermicity by 0.4 kcal/mol. Apparently, there is something missing in the chemical model used to calculate this value, and/or the methods are not totally adequate. It is in this context intriguing that the addition of O_2 is 1000 times slower in the absence of the B component and also that the reaction is strongly pH dependent. It is therefore clear that protonated complexes need to be investigated in future studies of this reaction.

The present mechanism of activating methane is consistent with isotope labeling experiments which show a large kinetic deuterium isotope effect[21] but is less in line with radical clock experiments which show very short radical lifetimes.[24,25] In the previous study using the smaller model, this was partly rationalized by a fast formation of an $Fe-CH_3$ bond immediately after the methane activation; see Scheme 1. Since the new model of compound **Q** in Figure 5 has 6-coordinated irons, this type of bond formation appears less plausible, although it cannot be entirely ruled out. Instead, the most obvious quenching of the methyl radical by the bridging OH group to form methanol remains the main alternative. Since this reaction is exothermic by as much as 63.0 kcal/mol and has no barrier, an unusually fast reaction might be possible. Steric effects of the protein, not considered here, might also play a role to accelerate this reaction. For example, if a bending of the methyl group in the region of the hydrogen abstraction transition state is forced by the protein, the methyl combination could become simpler. The energetics of such a process was tested by changing the O−C−H angle of the transition state in Figure 9 from 170 to 120°, while the O−H and C−H distances were kept fixed. The energy increase caused by this bending was about 6 kcal/mol, which is not negligible and argues somewhat against a direct bending of the transition state. The influence of the protein on the methyl group could, of course, also occur after the transition state is passed and still affect the methyl combination rate substantially.

Other models for a fast quenching of the radical were finally investigated. One rather obvious possibility is that the methyl radical forms a bond to one of the carboxylate ligands, Glu114 or Glu209, since these glutamates are very close to methane; see Figure 9. Indeed, this turns out to be the case, but the computed binding energy is quite large using the present model, which creates another problem of how methanol and not an ester can be formed if this bond is formed. One possibility could be that the methyl group could move from the carboxylate over to the bridging μ-OH group with only a small barrier. This possibility was tested in calculations, but the barrier appears to be rather high. The possibility that an intermediate water helps to bridge the carboxylate and μ-OH positions can be ruled out since this would imply that an oxygen from water would be incorporated into methanol, which contradicts experimental evidence.[21] It is interesting to note that a transfer of a hydrogen atom from a carboxylate over to a μ-bridging OCH_3 group occurs without any barrier. However, this type of transfer is not relevant if the hydrogen atom is not first abstracted by the carboxylate from methane. This type of mechanism was tested (see above) and was found to have a too high barrier. Instead, at the present stage, the very high methyl−carboxylate bond strength is concluded to be an artifact of the chemical model. It was already concluded above that if one of the carboxylate ligands becomes directly involved in bond formations, the model should ideally also include at least those second-sphere ligands that form hydrogen bonds directly to this carboxylate. Including such ligands (and there are experimental indications that there are very strong hydrogen bonds formed) should decrease the strength of the methyl bonds to the carboxylates substantially. Still, a quenching of the methyl radical by one of the carboxylate ligands remains only the second best suggestion to explain some of the radical clock experiments. An unusually fast methyl combination with the μ-bridging OH appears much more plausible.

d. Oxygen Activation. The activation of the oxygen molecule by the diiron complex turned out to be at least as difficult to describe computationally as the methane reaction. Starting from the asymmetric molecular O_2 minimum in Figure 8 and stretching the O−O bond in steps while optimizing all other degrees of freedom, a large number of unsuccessful attempts were made to locate a reasonably low transition state. Likewise, starting from compound **Q** in Figure 5 and moving the oxygens together did not lead to a low transition state either. It was not until one of the bridging carboxylates, Glu243, was moved over to one of the irons that the same approach started to yield

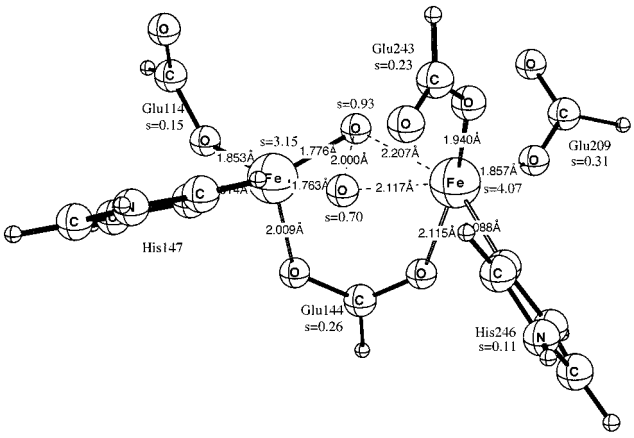

Figure 10. Optimized transition state for O_2 activation. The structure was obtained using ferromagnetic spin coupling (^{11}A).

reasonable energies. After different spin states were tried, the best state turned out to be the ferromagnetic ground state of compound **P**, ^{11}A. A suggested transition state is shown in Figure 10. Following this reaction path from the transition state by shortening the O−O distance further, and optimizing all other degrees of freedom, led to the structure in Figure 7, which is actually how this structure was initially located. It should be noted that an entirely proper transition state optimization was not successful, and the structure in Figure 10 is just the highest point on the reaction path followed. The barrier calculated from compound **P** in Figure 7 is 17.1 kcal/mol, corresponding to a rate of formation for compound **Q** of 1 s^{-1}, which is in reasonable agreement with experimental evidence.[2] However, it should be noted that this is a quite complicated transition state by computational standards and a case where the accuracy of the B3LYP method can be somewhat questioned. These difficulties are probably the main reason the proper full geometry optimization of the transition state failed.

The presently suggested pathway for the reaction of the diferrous reduced complex **1** with O_2 can be described in the following way. The first step is the formation of compound **P** in Figure 7, which occurs by first moving Glu243 (Glu238 for RNR) out of the way for O_2, making it monodentate to one of the irons. Moving the glutamate could lead to a minor barrier for this step, but this has not yet been investigated. The next step is the activation of O_2, which is accomplished by stretching the O−O bond on the ferromagnetically coupled ^{11}A surface while Glu243 is kept in a monodentate binding mode on one of the irons. When the oxygens have found their μ-oxo bridging positions, Glu243 can start to form its bridge between the irons. Finally, the spin is reduced to its antiferromagnetic coupling and compound **Q** in Figure 5 is formed.

Conclusions

In the present study using a larger model than previously for the iron dimer of RNR and MMO, several observed intermediates have been assigned possible structures. The full first ligand sphere was included in the model with four carboxylates and two imidazoles in overall neutral complexes. The present suggestions for compounds **Q** and **X** were based on the key experimental observation that the Fe−Fe distances of these intermediates are very short. It was found that a sufficiently short Fe−Fe distance for compound **Q** was reached when the irons were quadruply bridged by two μ-oxo groups and two bidentate carboxylates. By the placement of a hydrogen atom on one of the μ-oxo bridges, a suggestion for compound **X** was obtained with an almost as short Fe−Fe distance as for **Q**. Antiferromagnetic spin coupling was found to be quite important, shortening the Fe−Fe distance by about 0.2 Å compared to the ferromagnetic case. A symmetric peroxo structure was suggested for compound **P** where one of the bridging carboxylates of the reduced diferrous complex has moved to become monodentate on one of the irons to make place for O_2. The midpoint of O_2 was found to form a strongly bent angle of 132° with the two iron atoms in **P**.

A pure hydrogen abstraction transition state was found for methane activation by compound **Q**. A hydrogen atom was abstracted by the bridging μ-oxo group trans to the histidines, leading to the suggested model for compound **X** and a free methyl radical in an almost thermoneutral reaction. This type of transition state is consistent with large measured kinetic isotope effects and with experiments based on chiral substrates. Since the methyl combination reaction with the bridging μ-OH group was found to be very exothermic by 63 kcal/mol and had no barrier, it should be extremely fast and could explain some of the radical clock experiments, which failed to observe free radicals. It was suggested that parts of the protein not included in the present model could also have an important steric effect making the methyl combination even faster.

The activation of O_2 was found to occur by a symmetric stretching of the O−O bond on the ferromagnetic ground state surface of the suggested peroxo complex **P**. When the oxygens reached their final bridging μ-oxo positions, the reaction was completed by a closing of the second carboxylate bridge and a change of spin state leading to the quadruply bridged antiferromagnetic ground state of compound **Q**. This reaction has large similarities to the corresponding O_2 activation reaction previously found for a model of the dicopper complex of tyrosinase.[42] Both these reactions occur on a high-spin ground state of a bent peroxo complex by a symmetric stretching of the O−O bond until a planar bis(μ-oxo) structure is reached. At this point, the spin is reduced and the final complex is formed. However, the reverse of this reaction does not appear to have many similarities to the formation of O_2 in PSII, where both theory[48] and experiments[49] indicate that the oxygens forming the O−O bond are not identical and that an O_2H group is first formed before O_2 is finally obtained. Theory further indicates that an external water is involved in that case.

Acknowledgment. I am very grateful to Robert Crabtree for valuable comments on the paper.

IC981332W

(48) Siegbahn, P. E. M.; Crabtree, R. H. *J. Am. Chem. Soc.* **1999**, *121*, 117−127.
(49) Messinger, J.; Badger, M.; Wydrzinski, T. *Proc. Natl. Acad. Sci. U.S.A.* **1995**, *92*, 3209.